

Structure of the novel ternary hydrides  $\text{Li}_4\text{Tt}_2\text{D}$  ( $\text{Tt} = \text{Si}$  and  $\text{Ge}$ )

Hui Wu,<sup>a,b\*</sup> Michael R. Hartman,<sup>a,c</sup> Terrence J. Udovic,<sup>a</sup> John J. Rush,<sup>a,b</sup> Wei Zhou,<sup>a,d</sup> Robert C. Bowman Jr<sup>e</sup> and John J. Vajo<sup>f</sup>

<sup>a</sup>NIST Center for Neutron Research, National Institute of Standards and Technology, Gaithersburg, MD 20899-8562, USA,

<sup>b</sup>Department of Materials Science and Engineering, University of Maryland, College Park, MD 20742-2115, USA, <sup>c</sup>Department of Nuclear Engineering and Radiation Health Physics, Oregon State University, 116 Radiation Center, Corvallis, OR 97331-5903, USA, <sup>d</sup>Department of Materials Science and Engineering, University of Pennsylvania, 3231 Walnut Street, Philadelphia, PA 19104-6272, USA, <sup>e</sup>Jet Propulsion Laboratory, California Institute of Technology, Pasadena, CA 91109, USA, and <sup>f</sup>HRL Laboratories, LLC, Malibu, CA 90265, USA

Correspondence e-mail: huiwu@nist.gov

The crystal structures of newly discovered  $\text{Li}_4\text{Ge}_2\text{D}$  and  $\text{Li}_4\text{Si}_2\text{D}$  ternary phases were solved by direct methods using neutron powder diffraction data. Both structures can be described using a  $Cmmm$  orthorhombic cell with all hydrogen atoms occupying  $\text{Li}_6$ -octahedral interstices. The overall crystal structure and the geometry of these interstices are compared with those of other related phases, and the stabilization of this novel class of ternary hydrides is discussed.

Received 11 August 2006

Accepted 3 November 2006

## 1. Introduction

Light-metal hydrides such as  $\text{LiH}$  and  $\text{MgH}_2$  are promising candidates for hydrogen storage owing to their relatively high hydrogen-storage capacities. However, most of these hydrides have not been considered to be competitive because of rather slow absorption kinetics, relatively high thermal stability and/or problems with the reversibility of hydrogen absorption/desorption cycling. Altering the hydrogen-storage properties by hydride destabilization through alloy formation has recently attracted more attention. The strongly bound H atoms in  $\text{LiH}$  have been shown to be effectively destabilized *via* alloying with Si (Vajo *et al.*, 2004). Hydrogen absorption/desorption isotherm studies have indicated that several plateaus form for samples with different Li/Si ratios. The plateaus reflect the formation of distinct phases, most of them identified as known Li–Si intermetallic compounds (Bowman *et al.*, 2005). Yet, numerous additional X-ray diffraction (XRD) peaks in a hydrided sample with a 2.5:1 Li:Si ratio could not be assigned to any known Li– $\text{Tt}$  (tetrel;  $\text{Tt} = \text{Si}$ ,  $\text{Ge}$ ,  $\text{Sn}$  and  $\text{Pb}$ ) structure. NMR measurements suggested that these additional peaks represented the formation of a new Li–Si–H ternary phase (Bowman *et al.*, 2005).

Recently we discovered an analogous unknown phase during investigations of the  $\text{LiH/Ge}$  system and determined an approximate stoichiometry of  $\text{Li:Ge:H} \simeq 4:2:1$ . Here we report the structures of these ternary Li silicide and germanide hydrides with 4:2:1 stoichiometry, information which should contribute to an overall understanding of hydride destabilization in these and similar systems. The crystal structures were solved from neutron powder diffraction (NPD) data and will be discussed in light of the geometrical optimization of hydrogen-containing interstices and the stabilization of this new class of ternary hydrides.

## 2. Experimental

### 2.1. Synthesis of $\text{Li}_4\text{Si}_2\text{D}$ and $\text{Li}_4\text{Ge}_2\text{D}$

The  $\text{Li}_4\text{Ge}_2\text{D}$  powder sample was prepared by:

**Table 1**  
Rietveld summary for  $\text{Li}_4\text{Ge}_2\text{D}$  and  $\text{Li}_4\text{Si}_2\text{D}$ .

Chemical formula	$\text{Li}_4\text{Ge}_2\text{D}$	$\text{Li}_4\text{Si}_2\text{D}$
$T$ (K)	295	
Radiation type	Neutron	
Diffractometer	HRPD [Cu(311) monochromator, $\lambda = 1.5403$ (2)]	
Measured $2\theta$ range ( $^\circ$ )	3–165	
Cell setting, space group	Orthorhombic, $Cmmm$ (No. 65)	
$a$ ( $\text{Å}$ )	12.0030 (2)	11.9098 (6)
$b$ ( $\text{Å}$ )	3.87785 (5)	3.7625 (1)
$c$ ( $\text{Å}$ )	4.18199 (6)	4.1754 (2)
$V$ ( $\text{Å}^3$ )	194.655 (6)	187.106 (14)
$Z$	2	2
$R_{\text{wp}}$	0.0394	0.0585
$R_p$	0.0334	0.0486
$\chi^2$	1.000	1.977
$F_{\text{Li}_4\text{Ge}_2\text{D}}$ (wt%)	97.13 (1)	54.56 (4)
No. of measured and observed reflections	3188, 173	2764, 2618
No. of constraints†	6	6
Additional phase observed		
$F_{\text{LiD}}$ (wt%)	0.24 (1)	1.75 (8)
$a$ ( $\text{Å}$ )	4.0706 (3)	4.073 (1)
$F_{\text{Li}_2\text{D}}$ (wt%)	2.63 (7)	–
$a$ ( $\text{Å}$ )	4.6092 (1)	–
$F_{\text{Si}}$ (wt%)†	–	39.58 (3)
$a$ ( $\text{Å}$ )	–	5.42712 (8)
Si 8( $a$ ) (1/8, 1/8, 1/8) $U_{\text{iso}}$ ( $\times 100 \text{ Å}^2$ )	–	0.72 (3)
$F_{\text{Li}_2\text{Si}_7}$ (wt%)	–	4.11 (4)
$a, b, c$ ( $\text{Å}$ )	–	8.59576 (2), 19.7746 (1), 14.31889 (6)

† The anisotropic displacement parameters  $U^{ij}$  for Li atoms were constrained to be identical.

(i) evacuation of a ball-milled (400 r.p.m. for 50 min) LiH (Alfa Aesar<sup>2</sup> 99.4%) + Ge (Alfa Aesar, 99.999%) 9:4 stoichiometric mixture at 763 K for 8–10 h, and

(ii) deuteriding the resultant Li–Ge alloy by reaction with  $\sim 2.5$  MPa  $\text{D}_2$  (99.999%) at 723–743 K.

The compositions and structures of the products after each synthesis process were characterized using laboratory X-ray diffraction (Rigaku, D-MAX/UltimaIII) and neutron prompt-gamma activation analysis (PGAA; Lindstrom, 1993) techniques. Sample treatments were performed in a Mo foil pouch inside a stainless-steel tube. Sample handling was performed in a He-filled glovebox to avoid oxidation reactions. The stoichiometry of the resultant  $\text{Li}_y\text{Ge}_z\text{D}_x$  sample was determined by PGAA (Lindstrom, 1993) on a similarly prepared  $\text{Li}_y\text{Ge}_z\text{H}_x$  sample, which yielded an approximate ratio of  $\text{Li}:\text{Ge}:\text{H} \approx 4:2:1$ . The  $\text{Li}_4\text{Si}_2\text{D}$  powder sample was prepared using a procedure modified from the above to maximize  $\text{Li}_4\text{Si}_2\text{D}$  formation. First, an LiH (Fluka, 97%) + Si (cleaved from electronic grade wafers) 1:1 stoichiometric mixture was ball-milled (400 r.p.m. for 1 h; see Vajo *et al.*, 2004, for details) then evacuated at 773 K for 2–3 h to remove the hydrogen. Next, the LiSi alloy mixture was deuterided to a stoichiometry of  $\text{LiSiD}$  with  $\sim 0.7$  MPa of  $\text{D}_2$  (99.999%) at 723 K. Finally, a

<sup>2</sup> Certain commercial suppliers are identified in this paper to foster understanding. Such identification does not imply recommendation or endorsement by the NIST nor does it imply that the materials or equipment identified are necessarily the best available for the purpose.

portion of D was removed from the sample to a final ratio of 0.25 D:Li by controlled evacuation at 723 K followed by a 723 K annealing for 8–9 d in the sealed stainless-steel sample tube. The final sample composition was approximately  $\text{Li}_4\text{Si}_2\text{D} + 2\text{Si}$ , as determined by a combination of PGAA and NPD. The presence of excess Si was found to be necessary to promote the formation of  $\text{Li}_4\text{Si}_2\text{D}$  rather than of LiD.

## 2.2. Powder data collection

All NPD data were collected at the NIST Center for Neutron Research (NCNR, Gaithersburg, MD, USA) using the BT-1 high-resolution neutron powder diffractometer (Stalick *et al.*, 1995) with the Cu(311) monochromator at  $\lambda = 1.5403$  (2) Å and an in-pile collimation of 15 min of arc. Data were collected over the  $2\theta$  range 3–168° with a step size of 0.05°.

## 3. Results and discussion

### 3.1. Structural solution and refinement

The diffraction pattern of  $\text{Li}_4\text{Ge}_2\text{D}$  was indexed in an orthorhombic cell with  $a = 12.0030$  (2) Å,  $b = 3.8778$  (5) Å and  $c = 4.1819$  (6) Å (refined values; *CRYSFIRE*; Shirley, 2002), with indexing figure of merit:  $M(20) = 45$  (de Wolff, 1968). Evaluation of the systematic absences in the diffraction pattern indicated the space group  $Cmmm$  (No. 65). The XRD pattern from a hydride sample was first used to approximate the atomic positions for Ge and Li. D and Li positions were then determined from the NPD pattern of the deuteride sample with the fixed Ge positions obtained from the previous step. An *ab initio* structure determination using the *FOX* program (Favre-Nicolin & Cerny, 2002) in the  $Cmmm$  cell gave a best approximate crystal-structure solution and also yielded a stoichiometry of  $\text{Li}:\text{Ge}:\text{D} = 4:2:1$  in the unit cell. The stoichiometry of  $\text{Li}:\text{Ge}:\text{D} = 4:2:1$  was consistent with the PGAA results. Rietveld refinement of this structure model was then performed on the NPD pattern using the *GSAS* package (Larson & Von Dreele, 1994).

For  $\text{Li}_4\text{Ge}_2\text{D}$ , data in the 5–165°  $2\theta$  range were included comprising 173 Bragg reflections, which were described using a pseudo-Voigt peak-shape function (Thompson *et al.*, 1987). This function also included the microstrain broadening description (Stephens, 1999). The background was described by a ten-term Chebyshev polynomial function (*GSAS* type 1) throughout the whole pattern. The anisotropic displacement parameters for all atoms of the same element type were constrained to be identical for simplicity. Allowing for the independent refinement of displacement parameters for each atom in the unit cell led to similar structural results, with only a small increase in e.s.d. values of the displacement parameters. The diffraction pattern includes a small amount of a LiD

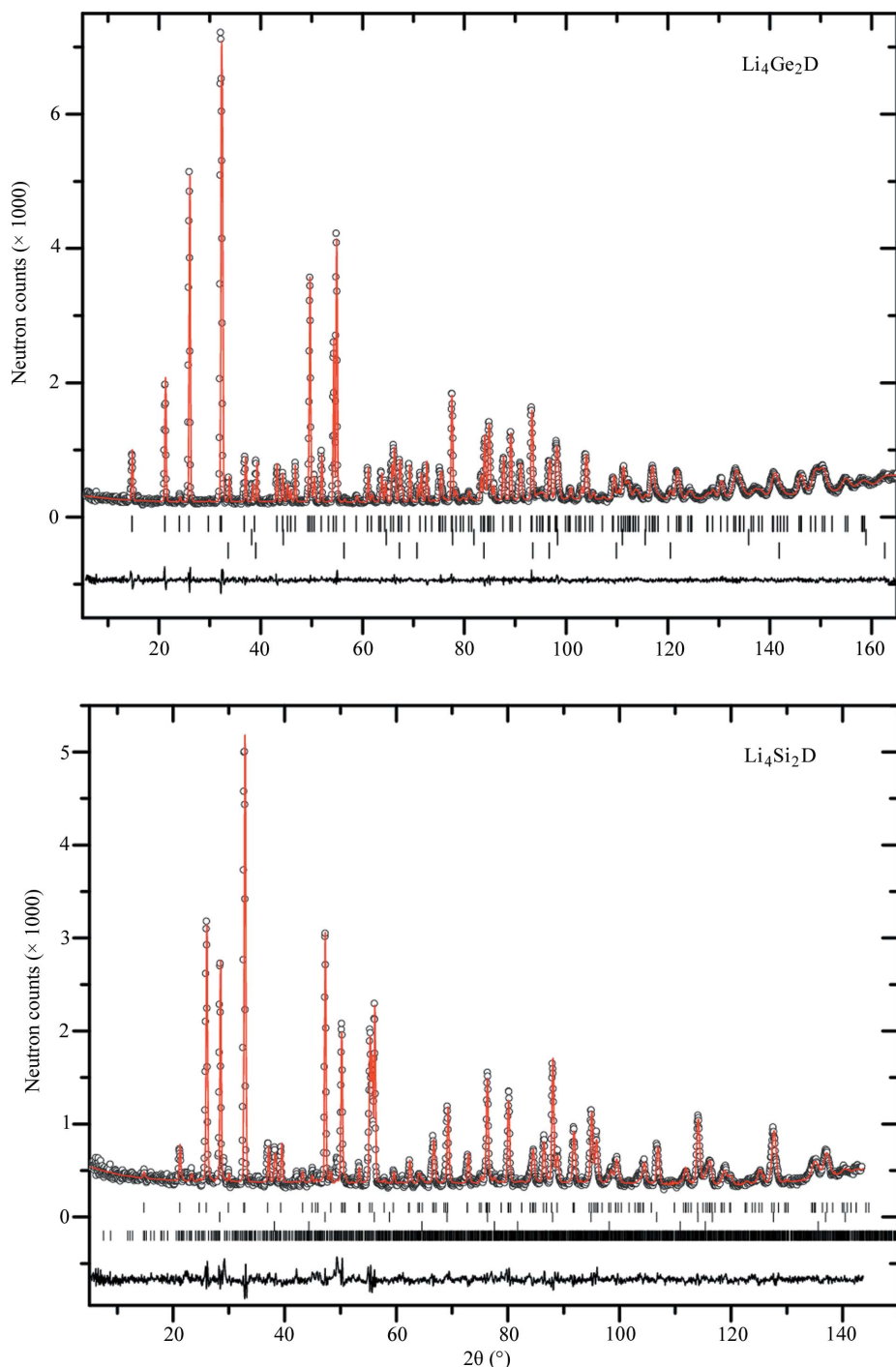


**Figure 1** Observed (circles), calculated (lines) and difference profiles of the Rietveld-refined NPD patterns for (a)  $\text{Li}_4\text{Ge}_2\text{D}$  and (b)  $\text{Li}_4\text{Si}_2\text{D}$ . Vertical bars indicate the calculated positions of Bragg peaks for (a)  $\text{Li}_4\text{Ge}_2\text{D}$ ,  $\text{LiD}$  and  $\text{Li}_2\text{O}$ , and (b)  $\text{Li}_4\text{Si}_2\text{D}$ ,  $\text{Si}$ ,  $\text{LiD}$  and  $\text{Li}_{12}\text{Si}_7$  (from the top).

phase with the NaCl-type structure, owing to the small excess of Li in the starting materials. The pattern also exhibits an additional set of weak lines corresponding to a small amount of a  $\text{Li}_2\text{O}$  phase, which may have been introduced by the impurities in the initial LiH precursor and/or the oxidized products from the extra LiH during the later heat-treatment

cycles. The refinement of 44 parameters including all these phases yielded final excellent agreement factors of  $R_{\text{wp}} = 0.0394$  and  $R_p = 0.0334$ .

For  $\text{Li}_4\text{Si}_2\text{D}$ , the diffraction pattern contains  $\text{Si}$  [39.58 (3) wt%],  $\text{LiD}$  [1.75 (8) wt%] and  $\text{Li}_{12}\text{Si}_7$  [4.11 (4) wt%] phases (refined fraction values). As for  $\text{Li}_4\text{Ge}_2\text{D}$ , the major phase can also be indexed using a  $Cmmm$  cell. This structure was refined following the procedure described above with the initial crystal-structure model for  $\text{Li}_4\text{Ge}_2\text{D}$ . There is a small fraction of an additional phase that can be neither identified using any of the currently known Li–Si compounds nor correlated to the reflections of the major  $\text{Li}_4\text{Si}_2\text{D}$  phase. Nonetheless, the refinement including these four phases still yielded reasonably good agreement factors. Detailed crystallographic information and final Rietveld refinement agreement factors for both structures are summarized in Tables 1 and 2.<sup>1</sup> Fig. 1 shows the final Rietveld plots for  $\text{Li}_4\text{Ge}_2\text{D}$  and  $\text{Li}_4\text{Si}_2\text{D}$ , respectively.

### 3.2. Discussion

Tables 1 and 2 list the atomic positions, displacement data and selected bond distances. The crystal structure of this new ternary hydride is illustrated for  $\text{Li}_4\text{Ge}_2\text{D}$  in Fig. 2. The structure type has two characteristic features:

- (i) interstitial octahedral sites defined by Li atoms around  $(\frac{1}{2}, \frac{1}{2}, \frac{1}{2})$   $(0, 0, \frac{1}{2})$  and
- (ii) an equal distribution of main-group tetrel anions aligned in a zigzag-chain fashion along the  $b$  direction in the basal planes ( $z = 0$ ).

Octahedral and tetrahedral interstitial H sites are both very common in transition-metal hydrides whose formulae are  $\text{MH}_2$  or  $\text{MH}_3$  (Udovic *et al.*, 1997), as well as in the alkali or alkaline-earth hydrides, *e.g.*  $\text{LiH}$  (NaCl-type),  $\text{MgH}_2$  ( $\text{TiO}_2$ -type) *etc.* However, for intermetallic metal hydrides, it is not that common to form single-element-defined octahedral sites.

<sup>1</sup> Supplementary data for this paper are available from the IUCr electronic archives (Reference: WS5053). Services for accessing these data are described at the back of the journal.

**Table 2**  
Structural parameters for  $\text{Li}_4\text{Ge}_2\text{D}$  and  $\text{Li}_4\text{Si}_2\text{D}$ .

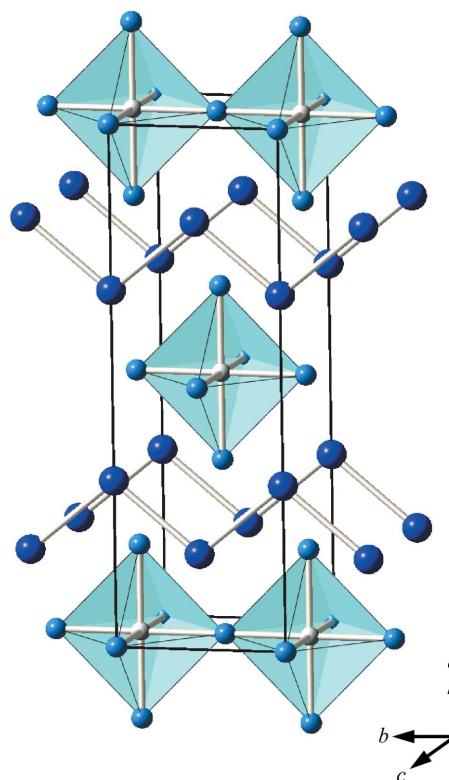
Atom	Site	Occupancy	$x$	$y$	$z$	$U^{11}$	$U^{22}$	$U^{33}$	$U^{12}$	$U^{13}$	$U^{13}$
<i>(a) Li<sub>4</sub>Ge<sub>2</sub>D</i>											
Ge	4( <i>g</i> )	1.00	0.3177 (1)	0	0	1.06 (4)	0.71 (3)	0.99 (3)	0	0	0
Li1	4( <i>h</i> )	1.00	0.8328 (2)	0	0.5	1.3 (1)	1.8 (1)	2.5 (1)	0	0	0
Li2	2( <i>c</i> )	1.00	0.5	0	0.5	1.3 (1)	1.8 (1)	2.5 (1)	0	0	0
Li3	2( <i>a</i> )	1.00	0	0	0	1.3 (1)	1.8 (1)	2.5 (1)	0	0	0
D	2( <i>d</i> )	0.967 (6)	0.5	0.5	0.5	1.89 (8)	1.44 (7)	2.44 (7)	0	0	0
<i>(b) Li<sub>4</sub>Si<sub>2</sub>D</i>											
Si	4( <i>g</i> )	1.00	0.3120 (2)	0	0	1.4 (1)	0.7 (1)	1.6 (2)	0	0	0
Li1	4( <i>h</i> )	1.00	0.8308 (5)	0	0.5	0.5 (1)	2.2 (3)	2.9 (3)	0	0	0
Li2	2( <i>c</i> )	1.00	0.5	0	0.5	0.5 (1)	2.2 (3)	2.9 (3)	0	0	0
Li3	2( <i>a</i> )	1.00	0	0	0	0.5 (1)	2.2 (3)	2.9 (3)	0	0	0
D	2( <i>d</i> )	0.927 (6)	0.5	0.5	0.5	2.7 (3)	1.7 (2)	1.6 (2)	0	0	0

Most of the reported octahedral interstices are comprised of mixed metals, *e.g.*  $\text{Fe}_4\text{R}_2$  octahedra in  $\text{R}_2\text{Fe}_{17}\text{H}(\text{N,C})_3$  compounds (*e.g.* Isnard *et al.*, 1990, 1992),  $\text{Na}_4\text{Mg}_2$  octahedra in  $\text{NaMgH}_3$  perovskite-type compounds and/or other ionic crystalline compounds such as alanates. The only examples so far reported containing octahedral sites defined by single elements are  $\text{Ti}_3\text{SnD}$  (Vennstrom *et al.*, 2004),  $\text{Mn}_3\text{SnD}$  (Grosse *et al.*, 1997) and  $\text{Ti}_5\text{Si}_3\text{D}_{0.9}$  (Kajitani *et al.*, 1986), where D locates in  $\text{Ti}_6$  or  $\text{Mn}_6$  octahedral interstices. Therefore, here the observation of  $\text{Li}_4\text{Ge}_2\text{D}$  and  $\text{Li}_4\text{Si}_2\text{D}$  compounds expands the known number in this ternary intermetallic hydride family. Interestingly, all these reported compounds contain main group tetrel (group IV<sub>A</sub>) elements.

Comparing the stoichiometries of this series of metal hydrides, it is notable that they all can be described using the general stoichiometry  $\text{A}_{2+n}\text{Tt}_n\text{D}$  ( $\text{Tt} = \text{Si, Ge and Sn}$ ). When  $n = 1$ ,  $\text{A}_3\text{TtD}_x$  (*e.g.*  $\text{Ti}_3\text{SnD}$ ) at low D concentration forms an orthorhombic ( $\text{C}222_1$ ) structure with face-shared  $\text{A}_6$  octahedra. For  $\text{Ti}_3\text{SnD}$ , this structure will transform to a cubic ( $\text{Pm}\bar{3}m$ ) structure containing corner-shared  $\text{Ti}_6$  octahedra at  $x = 1$  through a hexagonal  $\text{Ti}_3\text{Sn}$  meta phase. First-principles calculations suggest that the H–H distances in these two polymorphs are very important for the phase transition upon hydrogenation (Vennstrom *et al.*, 2004). When  $n = 2$ ,  $\text{A}_4\text{Tt}_2\text{D}$  (*e.g.*  $\text{Li}_4\text{Ge}_2\text{D}$  in the current study) forms an orthorhombic  $\text{Cmmm}$  structure with corner-shared octahedra. This crystalline phase can be viewed as a transformation from the cubic  $\text{Ti}_3\text{SnD}$  structure *via* a doubling of the **a** axis, plus a parallel glide of  $\text{Li}_6$ -octahedral layers along **b** for  $y = \frac{1}{2}$ . For  $n = 3$  we have  $\text{A}_5\text{Tt}_3\text{D}_{0.9}$ , *e.g.*  $\text{Ti}_5\text{Si}_3\text{D}_{0.9}$ , which was reported to have a hexagonal structure with face-shared  $\text{Ti}_6$  octahedra. It can also be viewed as an orthorhombic structure analogous to the  $n = 1$  orthorhombic  $\text{Ti}_3\text{SnD}_x$  ( $x < 1$ ) with the lattice parameters  $a_o = a_h$ ,  $b_o = 3^{1/2}a_h$ ,  $c_o = c_h$ . In fact,  $\text{Ti}_5\text{Si}_3\text{D}_{0.9}$  is the only example with the  $\text{A}_5\text{Tt}_3$  stoichiometry containing octahedral H sites. All the other reported  $\text{A}_5\text{Tt}_3$  ( $\text{A} = \text{Ca, Sr, Ba, Tt} = \text{Si, Ge, Sn}$ ) intermetallic compounds form  $\text{Cr}_5\text{B}_3$ -type binary and ternary hydride or fluoride phases with tetrahedral interstitial sites (Leon-Escamilla & Corbett, 2001). The tetrahedral site occupation in these systems may occur in a similar way to orthorhombic  $\text{Ti}_3\text{SnD}_x$  ( $x < 1$ ; Vennstrom *et al.*, 2004), where

the octahedra are so distorted and the octahedral cavities so large that the D atoms prefer the energetically more favorable  $\text{Ti}_4$  sites. Finally, it should be mentioned that the  $n = 0$  compounds (*i.e.*  $\text{A}_2\text{D}$ ) have also been reported containing the  $\text{A}_6$ -octahedral H sites such as monoclinic  $\beta\text{-V}_2\text{D}$  under no stress and tetragonal  $\beta_1\text{-V}_2\text{H}$  with stress-induced hydrogen ordering (Noda *et al.*, 1985). The structure variations in the  $\text{A}_{2+n}\text{Tt}_n\text{D}$  series compounds are illustrated in Figs. 3 and 4.

Another significant feature in these novel  $\text{Li}_4\text{Ge}_2\text{D}$  and  $\text{Li}_4\text{Si}_2\text{D}$  structures is the formation of the long-range –Ge–Ge– or –Si–Si– chains with Ge–Ge and Si–Si bond

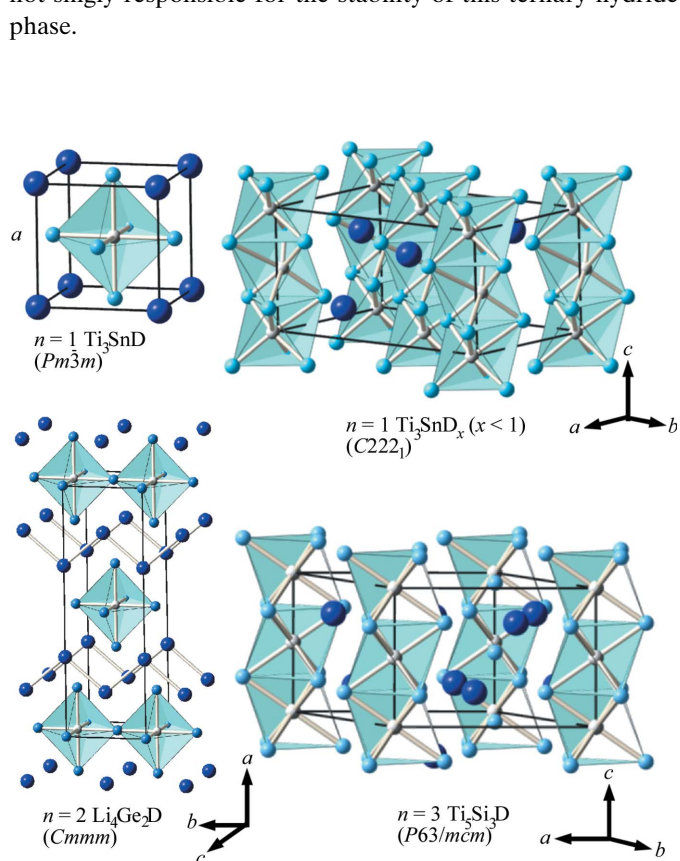


**Figure 2**  
An off-[001] view of the orthorhombic  $\text{Li}_4\text{Ge}_2\text{D}$  crystal structure with centered octahedral interstices. The large dark and small light spheres represent Ge and Li, respectively, and the interstitial D atoms are centered in the shaded  $\text{Li}_6$  octahedra.

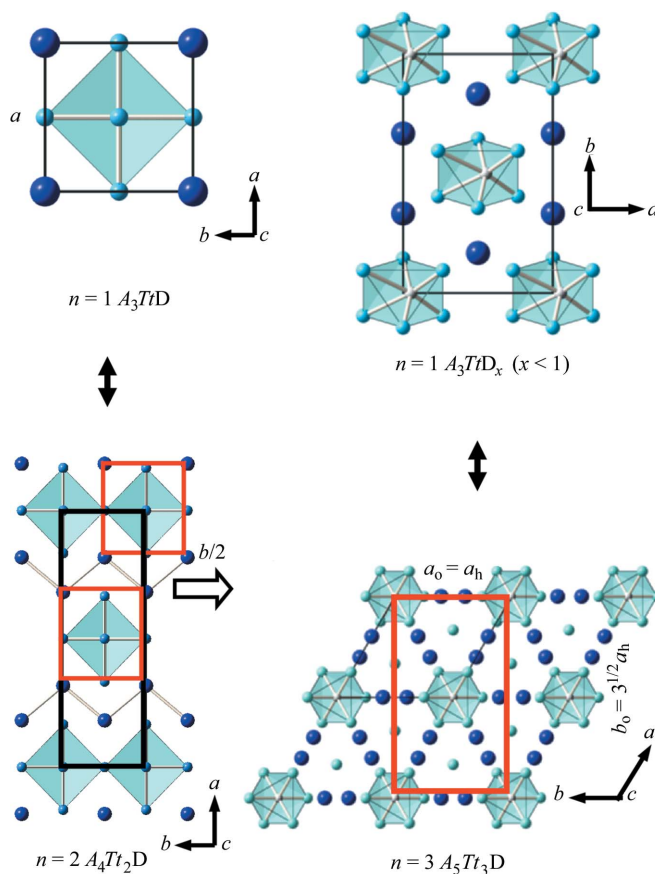
**Table 3**  
 Important atomic distances (Å) in  $\text{Li}_4\text{Ge}_2\text{D}$  and  $\text{Li}_4\text{Si}_2\text{D}$ .

$\text{Li}_4\text{Ge}_2\text{D}$		$\text{Li}_4\text{Si}_2\text{D}$	
D—Li1 2×	2.0077 (29)	D—Li1 2×	2.016 (6)
D—Li2 2×	1.93893 (3)	D—Li2 2×	1.88126 (8)
D—Li3 2×	2.09100 (3)	D—Li3 2×	2.08772 (11)
D1—D1	3.87785 (5)	D1—D1	3.76253 (16)
Ge1—Ge1	2.5300 (10)	Si1—Si1	2.391 (4)
Ge1—Li1 2×	2.7628 (19)	Si1—Li1 2×	2.692 (4)
Ge1—Li1 4×	2.85732 (19)	Si1—Li1 4×	2.8191 (6)
Ge1—Li2 2×	3.0266 (6)	Si1—Li2 2×	3.0615 (25)
Ge1—Li3 2×	2.9236 (6)	Si1—Li3 2×	2.9246 (26)

distances of  $\sim 2.53$  and  $\sim 2.39$  Å, which are much longer than the isolated  $Tt$ — $Tt$  dimeric units in binary  $\text{Li}$ — $Tt$  phases, e.g. 2.44–2.47 Å in  $\text{Li}_9\text{Ge}_4$  (Hopf *et al.*, 1970) and  $\text{Li}_{11}\text{Ge}_9$  (Frank & Mueller, 1975), 2.33–2.35 Å in  $\text{Li}_7\text{Si}_3$  (von Schnering *et al.*, 1980) and  $\text{Li}_{12}\text{Si}_7$  (Nesper *et al.*, 1986). These distances are comparable to those in the dimeric units in  $\text{Ca}_5\text{Ti}_3$  and  $\text{Ca}_5\text{Ti}_3\text{H}_x$  (Leon-Escamilla & Corbett, 2001),  $\sim 2.57$  and 2.45 Å, and to those in the similarly bonded clathrate II network structures  $A_8A'_6Tt_{136}$  (Ge—Ge 2.49–2.51 and Si—Si 2.36–2.39 Å; Bobev & Sevov, 2000). Therefore, the formation of the  $Tt$ — $Tt$  chain and the range of  $Tt$ — $Tt$  bond distances are not singly responsible for the stability of this ternary-hydride phase.


**Figure 3**  
 Crystal structures of  $A_{2+n}T_n\text{D}$  series compounds.  $n = 1$ :  $\text{Ti}_3\text{SnD}$  ( $Pm\bar{3}m$ ) and  $\text{Ti}_3 > \text{SnD}_x$  ( $x < 1$ ) ( $C222_1$ );  $n = 2$ :  $\text{Li}_4\text{Ge}_2\text{D}$  and  $\text{Li}_4\text{Si}_2\text{D}$  ( $Cmmm$ );  $n = 3$ :  $\text{Ti}_3\text{Sn}_3\text{D}$  ( $P63/mcm$ ). The large dark and small light spheres represent  $Tt$  and  $A$ , respectively, and the interstitial D atoms are centered in the shaded  $\text{Li}_6$  octahedra.

In all known  $\text{Li}$ — $Tt$  systems (Hopf *et al.*, 1970; Frank & Mueller, 1975; von Schnering *et al.*, 1980; Frank *et al.*, 1975; Nesper *et al.*, 1986) atoms are closely packed with no tetrahedral or octahedral sites large enough for hydrogen inclusion. In the  $\text{Li}_4Tt_2\text{D}$  structure, the  $\text{Li}$ — $\text{H}$  bond lengths (see Table 3) are comparable to those in pure  $\text{LiH}$  ( $\text{Li}$ — $\text{H}$  2.031 Å; Calder *et al.*, 1962), indicating quite strong  $\text{Li}$ — $\text{H}$  bonding. We noted that the shortest  $\text{Ge}$ — $\text{Li}$  and  $\text{Si}$ — $\text{Li}$  distances are  $\sim 2.76$  and  $\sim 2.69$  Å, respectively, which are significantly lengthened compared with the shortest  $\text{Li}$ — $Tt$  distances in binary  $\text{Li}$ — $\text{Ge}$  and  $\text{Li}$ — $\text{Si}$  phases, e.g.  $\sim 2.53$ – $2.55$  Å in  $\text{Li}_{11}\text{Ge}_9$  (Frank & Mueller, 1975) and  $\text{Li}_9\text{Ge}_4$  (Hopf *et al.*, 1970),  $\sim 2.52$ – $2.59$  Å in  $\text{Li}_{13}\text{Si}_4$  (Frank *et al.*, 1975),  $\text{Li}_7\text{Si}_3$  (von Schnering *et al.*, 1980) and  $\text{Li}_{12}\text{Si}_7$  (Nesper *et al.*, 1986). Therefore, the interactions between  $\text{Li}$  and  $Tt$  atoms are much weakened, leading to the existence of possible interstitial sites. Assuming the absence of interstitial H in the present ternary structure,  $\text{Li}$  atoms would have to approach the  $Tt$  atoms so as to shorten the  $\text{Li}$ — $Tt$  distances and decrease the overall energy. Consequently, this outward movement of  $\text{Li}$  atoms would expand the octahedral cavities and make them too large to be energetically favorable. Note that there is no 2:1  $\text{Li}_2Tt$  composition forming a binary phase with empty octahedra for any  $Tt = \text{Si}$ ,  $\text{Ge}$  or  $\text{Sn}$  system.


**Figure 4**  
 Structure comparison of  $A_{2+n}T_n\text{D}$  series compounds projected in the  $[001]$  direction. The large dark and small light spheres represent  $Tt$  and  $A$ , respectively, and the interstitial D atoms are centered in the shaded  $\text{Li}_6$  octahedra.

Therefore, we believe the strong Li–H bonding and an appropriate sizing of the nearest-neighbor Li and *Tt*, as well as the existence of interstitial sites are primarily responsible for the stabilities of these ternary hydrides.

### 4. Summary

Using NPD, we have solved the crystal structure of a new class of ternary hydrides possessing the stoichiometry  $\text{Li}_4\text{Tt}_2\text{D}$  (*Tt* = Si and Ge). The structure is described using an orthorhombic unit cell with space group *Cmmm* and contains a single type of hydrogen in  $\text{Li}_6$  octahedral interstices, which is consistent with previous NMR results. The instabilities of binary ‘ $\text{Li}_2\text{Tt}$ ’ for *Tt* = Si and Ge with empty octahedral sites and their stabilities as ternary hydrides with interstitial binding are related to the appropriate distances of the nearest Li and *Tt* and the size of the  $\text{Li}_6$  octahedral cavities. The discovery of this new structure class expands the number of ternary hydride phases containing hydrogen in single-element octahedral interstices.

We would like to thank Dr A. Santoro for his valuable comments on this paper and Dr C. C. Ahn for his structural insights during the early stages of this investigation. This work was partially supported by DOE through EERE Grant Nos. DE-AI-01-05EE11104, DE-AI-01-05EE11105 and DE-FC36-05GO15067, and BES Grant No. DE-FG02-98ER45701. This research was partially performed at the Jet Propulsion Laboratory, which is operated by the California Institute of Technology under contract with the NASA.

### References

- Bobev, S. & Sevov, S. C. (2000). *J. Solid State Chem.* **153**, 92–105.
- Bowman Jr, R. C., Hwang, S.-J., Ahn, C. C. & Vajo, J. J. (2005). *Mater. Res. Soc. Symp. Proc.* **837**, 3.6.1–3.6.6.
- Calder, R. S., Cochran, W., Griffiths, D. & Lowde, R. D. (1962). *J. Phys. Chem. Solids*, **23**, 621–632.
- Favre-Nicolin, V. & Cerny, R. J. (2002). *J. Appl. Cryst.* **35**, 734–743.
- Frank, U. & Mueller, W. (1975). *Z. Naturforsch. Teil B*, **30**, 313–315.
- Frank, U., Mueller, W. & Schaefer, H. (1975). *Z. Naturforsch. Teil B*, **30**, 10–13.
- Grosse, G., Wagner, F. E., Antonov, V. E. & Antonova, T. E. (1997). *J. Alloys Compd.* **253**, 339–342.
- Hopf, V., Schaefer, H. & Weiss, A. (1970). *Z. Naturforsch. Teil B*, **25**, 653–653.
- Isnard, O., Miraglia, S., Soubeyroux, J. L. & Fruchart, D. (1990). *J. Less-Common Met.* **162**, 273–284.
- Isnard, O., Miraglia, S., Soubeyroux, J. L. & Fruchart, D. (1992). *Solid State Commun.* **81**, 13–19.
- Kajitani, T., Kawase, T., Yamada, K. & Hirabayashi, M. (1986). *Trans. Jpn Inst. Met.* **27**, 639–647.
- Larson, A. C. & Von Dreele, R. B. (1994) *GSAS*, Report LAUR 86-748. Los Alamos National Laboratory, New Mexico, USA.
- Leon-Escamilla, E. A. & Corbett, J. D. (2001). *J. Solid State Chem.* **159**, 149–162.
- Lindstrom, R. M. (1993). *J. Res. Natl. Inst. Stand. Technol.* **98**, 127–133.
- Nesper, R., von Schnering, H. G. & Curda, J. (1986). *Chem. Ber.* **119**, 3576–3590.
- Noda, Y., Kajitani, T., Hirabayashi, M. & Sato, S. (1985). *Acta Cryst.* **C41**, 1566–1571.
- Schnering, H. G. von, Nesper, R., Tebbe, K. F. & Curda, J. (1980). *Z. Metall.* **71**, 357–363.
- Shirley, R. (2002). *The CRYSFIRE System for Automatic Powder Indexing: User's Manual*. Guildford: The Lattice Press.
- Stalick, J. K., Prince, E., Santoro, A., Schroder, I. G. & Rush, J. J. (1995). *Neutron Scattering in Materials Science*, edited by D. A. Neumann, T. P. Russell & B. J. Wuensch, Vol. II. Mater. Res. Soc. Symp. Proc. No. 376, p. 101. Materials Research Society, Pittsburgh, PA.
- Stephens, P. (1999). *J. Appl. Cryst.* **32**, 281–289.
- Thompson, P., Cox, D. E. & Hastings, J. B. (1987). *J. Appl. Cryst.* **20**, 79–83.
- Udovic, T. J., Rush, J. J., Huang, Q. & Anderson, I. S. (1997). *J. Alloys Compd.* **253–254**, 241–247.
- Vajo, J. J., Mertens, F., Ahn, C. C., Bowman Jr, R. C. & Fultz, B. (2004). *J. Phys. Chem. B*, **108**, 13977–13983.
- Vennstrom, M., Grechnev, A., Eriksson, O. & Andersson, Y. (2004). *J. Alloys Compd.* **364**, 127–131.
- Wolff, P. M. de (1968). *J. Appl. Cryst.* **1**, 108–113.